Inorg. Chem. **2004**, *43*, 3230–3236

Unusually High Chemical Compressibility of Normally Rigid Type-I Clathrate Framework: Synthesis and Structural Study of $Sn_{24}P_{19.3}Br_xI_{8-x}$ Solid Solution, the Prospective Thermoelectric Material

Kirill A. Kovnir,[†,‡] Julia V. Zaikina,[‡] Lyudmila N. Reshetova,[‡] Andrei V. Olenev,[‡] Evgeny V. Dikarev,[§] and Andrei V. Shevelkov*[,‡]

Department of Materials Sciences and Inorganic Synthesis Laboratory, Department of Chemistry, Moscow State University, Moscow 119992, Russia, and Department of Chemistry, University at Albany, Albany, New York 12222

Received September 17, 2003

A novel tin phosphide bromide, $Sn_{24}P_{19.3(2)}Br_8$, and $Sn_{24}P_{19.3(2)}Br_xI_{8-x}$ ($x = 0$–8) solid solution have been prepared and structurally characterized. All compounds crystallize with the type-I clathrate structure in the cubic space group $Pm\bar{3}n$ (No. 223). The clathrate framework of the title solid solution shows a remarkable chemical compressibility: the unit cell parameter drops from 10.954(1) to 10.820(1) Å on going from $x = 0$ to $x = 8$, a feature that has never been observed for normally rigid clathrate frameworks. The chemical compressibility as well as non-Vegard dependence of the unit cell parameter upon the bromine content is attributed to the nonuniform distribution of the guest halogen atoms in the polyhedral cavities of the clathrate framework. The temperature-dependent structural study performed on $Sn_{24}P_{19.3(2)}Br_8$ has shown that, in contrast to the chemical compressibility, the thermal compressibility (linear contraction) of the phase is similar to that observed for the Group 14 anionic clathrates. The tin phosphide bromide does not undergo phase transition down to 90 K, and the atomic displacement parameters for all atoms decrease linearly upon lowering the temperature. These linear dependencies have been used to assess such physical constants as Debye temperature, 220 K, and the lattice part of thermal conductivity, 0.7 W/(m K). Principal differences between the title compounds and the group 14 anionic clathrates are highlighted, and the prospects of creating new thermoelectric materials based on cationic clathrates are briefly discussed.

Introduction

A large family of inclusion compounds characterized by a complete sequestering of guest particles by a host framework is known as the clathrates.[1] The term clathrate first used in 1948 by Powell[2] to identify organic inclusion compounds was expanded on gas hydrates by Pauling who solved the crystal structure of the chlorine hydrate.[3] The polar intermetallics having the structure of the chlorine hydrates, also known as the clathrate-I structure type, were discovered shortly after.[4,5] The majority of these compounds exhibit properties of narrow gap semiconductors and, in general, Zintl phases,[6] and the term semiconducting clathrates is now accepted in the literature.[7] Semiconducting clathrates are typically anionic as their frameworks are composed of group 13−14 metals acquiring electrons from group 1−2 metals or europium, which serve as guests. That type of clathrate is surveyed briefly in a microreview.[8] The semiconducting clathrates with the reversed host−guest polarity are also known;[9−14] the structure of a typical cationic[15] clathrate, $Sn_{24}P_{19.3}I_8$,[12] is shown in Figure 1.

* To whom correspondence should be addressed. E-mail: shev@inorg.chem.msu.ru. Fax: (+7-095) 939 47 88.

† Department of Materials Sciences, Moscow State University.

‡ Inorganic Synthesis Laboratory, Department of Chemistry, Moscow State University.

§ University at Albany.

(1) Wells, A. F. *Structural Inorganic Chemistry*, 5th Ed.; Clarendon Press: Oxford, 1986; Chapter 15.
(2) Powell, H. *J. Chem. Soc.* **1948**, *45*, 61−73.
(3) Pauling, L.; Marsh, R. E. *Proc. Natl. Acad. Sci.* **1952**, *36*, 112−118.
(4) Cros, C.; Pouchard, M.; Hagenmuller, P. *C. R. Acad. Sci.* **1965**, *260*, 4764−4797.
(5) Kasper, J. S.; Hagenmuller, P.; Pouchard, M. *Science*. **1965**, *150*, 1713−1714.
(6) (a) Miller, G. J. In *Chemistry, Structure, and Bonding of Zintl Phases and Ions*; Kauzlarich, S. M., Ed.; VCH: New York, 1996; pp 1−59. (b) Corbett, J. D. In *Chemistry, Structure, and Bonding of Zintl Phases and Ions*; Kauzlarich, S. M., Ed.; VCH: New York, 1996; pp 139−181.
(7) Müller, A.; Reuter, H.; Dillinger, S. *Angew. Chem., Int. Ed. Engl.* **1995**, *34*, 2328−2361.
(8) Bobev, S.; Sevov, S. C. *J. Solid State Chem.* **2000**, *153*, 92−105.

10.1021/ic035097f CCC: $27.50
Published on Web 04/14/2004

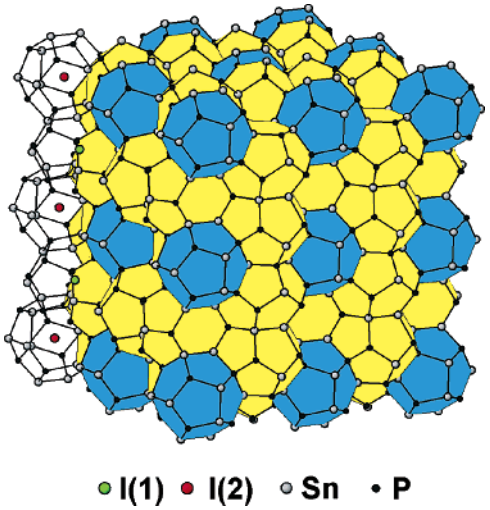

Figure 1. A view of the crystal structure of $Sn_{24}P_{19.3}I_8$, a representative cationic clathrate. Dodecahedra around the I(1) atoms are shown in blue; tetrakaidecahedra around the I(2) atoms are shown in yellow.

Semiconducting clathrates with the type-I structure based on the group 14 elements trigger growing interest due to expectations that thermoelectric materials of new generation will emerge following the guidelines of the "phonon glass, electron crystal" concept.[16,17] The intensive studies of all aspects of their chemistry and physics, including synthesis, crystal and electronic structure, phase transitions, magnetic behavior, and transport properties have been documented in a number of recent papers.[13,14,18−29] One of the structural features under discussion[14,18,23,25,27,29] is the "rattling" of the guest atoms in the oversized clathrate cages of the type-I structure, which is believed to reduce thermal conductivity, thus improving thermoelectric properties. The analysis of literature data shows that the rattling is sensitive to the host−guest mismatch and cannot be effectively optimized since the clathrate framework is very rigid.

In this work, we report the synthesis and X-ray diffraction study of a novel clathrate $Sn_{24}P_{19.3(2)}Br_8$, which turned out to be isostructural with the previously reported $Sn_{24}P_{19.3}I_8$,[12] and a solid solution $Sn_{24}P_{19.3(2)}Br_xI_{8-x}$. This system shows a very high chemical compressibility of the clathrate framework. The dependence of the unit cell dimensions upon the composition and its influence on bonding, as well as the distribution of the guest atoms in two different polyhedral cages of the clathrate framework, are discussed. Temperature-dependent structural data are used for the first time to assess some physical constants of a novel cationic clathrate.

Experimental Section

Starting Materials. Metallic tin and crystalline iodine (Reakhim, 99.99%) were used as received. Red phosphorus (Reakhim, 97%) was purified by washing consecutively with 30% aqueous solution of KOH, water, ethanol, and diethyl ether (twice) and then vacuum-dried. Tin(IV) iodide was synthesized by the reaction of excess tin with iodine in CCl_4 according to literature data.[30] To synthesize tin(II) bromide, metallic tin was first treated with concentrated hydrobromic acid in the presence of metallic platinum as a catalyst. After completion of the reaction, the solvent was evaporated to yield yellow crystals that were dried over P_2O_5 for 24 h. The dried crystals, adduct of tin dibromide and hydrobromic acid of variable composition, were then decomposed in Ar atmosphere, and the residue was heated in a sealed silica tube with the addition of an approximately equivoluminal quantity of metallic tin at 500 °C for 72 h. The product appeared as solidified colorless melt and was mechanically separated from the residual tin. An X-ray powder analysis confirmed it to be pure $SnBr_2$.

Physical Methods. Guinier type FR-552 chamber (Nonius) operated with the Ge-monochromatized Cu Kα radiation was used for the phase analysis and unit cell parameter determination. The purity of the samples was checked by the profile analysis of the diffractograms recorded with STADI-P (Stoe) X-ray powder diffractometer working on Cu Kα radiation in a transmission mode. Microprobe analysis was performed with JEOL JSN-840A scanning electron microscope equipped with the PGT IMIX analyzer. Magnetic susceptibility was measured using a standard Faraday balance. Resistivity measurements were performed on pressed pellets using a standard 4-probe device.

Synthesis and X-ray Characterization. Samples with the overall $Sn_{24}P_{19.3(2)}Br_xI_{8-x}$ ($x = 0, 1, 2, 3, 4, 5, 6, 7, 8$) composition were prepared by heating the respective stoichiometric mixtures of tin, red phosphorus, tin(IV) iodide, and tin(II) bromide in sealed

(9) von Schnering, H. G.; Menke, H. *Angew. Chem.* **1972**, *84*, 30−31.
(10) Menke, H.; von Schnering, H. G. *Z. Anorg. Allg. Chem.* **1973**, *395*, 223−238.
(11) Nesper, R.; Curda, J.; von Schnering, H. G. *Angew. Chem., Int. Ed. Engl.* **1986**, *25*, 350−352.
(12) Shatruk, M. M.; Kovnir, K. A.; Shevelkov, A. V.; Presniakov, I. A.; Popovkin, B. A. *Inorg. Chem.* **1999**, *38*, 3455−3457.
(13) Shatruk, M. M.; Kovnir, K. A.; Lindsjö, M.; Presniakov, I. A.; Kloo, L. A.; Shevelkov, A. V. *J. Solid State Chem.* **2001**, *161*, 233−242.
(14) Reshetova, L. N.; Zaikina, J. V.; Shevelkov, A. V.; Kovnir, K. A.; Lindsjö, M.; Kloo, L. *Z. Anorg. Allg. Chem.* **2002**, *628*, 2145.
(15) The term "cationic clathrates" reflects the total positive charge smeared over the polyhedral framework to compensate for the charge of guests. Other terms used in the literature instead of "cationic clathrates" are "polycationic clathrates" and "inverse clathrates".[6,7,14]
(16) Slack, G. A. In *CRC Handbook of Thermoelectrics*; Rowe, D. M., Ed.; CRC Press: Boca Raton, FL, 1995.
(17) Nolas, G. S.; Slack, G. A.; Schjuman, S. B. In *Recent Trends in Thermoelectric Materials Research*; Tritt, T. M., Ed.; Academic Press: San Diego, CA, 2001.
(18) Paschen, S.; Pacheco, V.; Bentien, A.; Sanchez, A.; Carrillo-Cabrera, W.; Baenitz, M.; Iversen, B. B.; Grin, Yu.; Steglich, F. *Physica B* **2003**, *328*, 39−43.
(19) Mudryk, Ya.; Rogl, P.; Paul, C.; Berger, S.; Bauer, E.; Hilscher, G.; Godart, C.; Noël, H.; Saccone, A.; Ferro, R. *Physica B* **2003**, *328*, 44−48.
(20) Leoni, S.; Carrillo-Cabrera, W.; Grin, Yu. *J. Alloys Compd.* **2003**, *350*, 113−122.
(21) Mollnitz, L.; Blake, N. P.; Metiu, H. *J. Chem. Phys.* **2002**, *117*, 1302−1312.
(22) Wilkinson, A. P.; Lind, C.; Young, R. A.; Shastri, S. D.; Lee, P. L.; Nolas, G. S. *Chem. Mater.* **2002**, *14*, 1300−1305.
(23) Sales, B. C.; Chakoumakos, B. C.; Jin, R.; Thompson, J. R.; Mandrus, D. *Phys. Rev. B* **2001**, *63*, 245113/1−245113/8.
(24) Paschen, S.; Carrilo-Cabrera, W.; Bentien, A.; Tran, V. H.; Baenitz, M.; Grin, Yu.; Steglich, F. *Phys. Rev. B* **2001**, *64*, 214404/1−214404/11.
(25) Chakoumakos, B. C.; Sales, B. C.; Mandrus, D. G. *J. Alloys Compd.* **2001**, *322*, 127−134.
(26) Iversen, B. B.; Palmqvist, A. E. C.; Cox, D. E.; Nolas, G. S.; Stucky, G. D.; Blake, N. P.; Metiu, H. *J. Solid State Chem.* **2000**, *149*, 455−458.
(27) Chakoumakos, B. C.; Sales, B. C.; Mandrus, D. G.; Nolas, G. S. *J. Alloys Compd.* **2000**, *296*, 80−86.
(28) Ramachandran, G. K.; McMillan, P. F.; Dong, J.; Sankey, O. F. *J. Solid State Chem.* **2000**, *154*, 626−634.
(29) Nolas, G. S.; Chakoumakos, B. C.; Mahieu, B.; Long, G. J.; Weakley, T. J. R. *Chem. Mater.* **2000**, *12*, 1947−1953.
(30) *Handbuch der Präparativen Anorganischen Chemie*; Brauer, G., Ed.; Ferdinand Enke Verlag: Stuttgart, 1975.

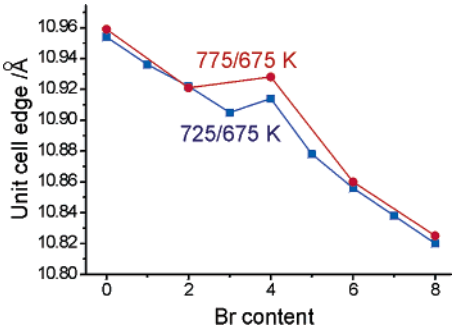

Figure 2. Dependence of the cubic unit cell parameter of $Sn_{24}P_{19.3(2)}Br_xI_{8-x}$ on the bromine content for the samples annealed at different temperatures. Solid lines are drawn to guide an eye. The esd's are smaller than the symbols used for the experimental data on this graph.

silica tubes under vacuum at 725 K for 5 days. The samples were then reground and heated again in evacuated silica tubes at 675 K for another 14 days, and then furnace-cooled to room temperature. After the second annealing, the samples appeared as black air-stable homogeneous polycrystalline powders. An X-ray analysis showed that in all cases the diffraction patterns were isomorphous to that of the previously reported[12] cubic clathrate-I phase $Sn_{24}P_{19.3}I_8$. However, the systematic shift of the lines on the Guinier photos was observed, and the traces of the binary tin phosphide, Sn_4P_3, were also detected for the samples rich in bromine content. All lines, except those of Sn_4P_3, were indexed in a cubic system by analogy with $Sn_{24}P_{19.3}I_8$. The calculated unit cell parameters are plotted against the bromine content in Figure 2. The second series of the samples with $x = 0$, 2, 4, 6, and 8 was prepared under the same conditions, save for the first annealing temperature that was set at 775 K; the results are shown in Figure 2. As the traces of the impurity phase Sn_4P_3 were observed, the reproducibility of the obtained results was checked. Each series of the experiments was reproduced twice. The resulting unit cell parameters were the same for a sample with the same starting composition, the difference being not greater than 0.002 Å, which is only twice larger than the esd.

Single-Crystal Preparation. To investigate the features of the crystal structures, the single crystals of the following composition were obtained: $Sn_{24}P_{19.2(1)}Br_{2.35(3)}I_{5.65(3)}$ (**I**), $Sn_{24}P_{19.1(1)}Br_{3.14(4)}I_{4.86(4)}$ (**II**), $Sn_{24}P_{19.2(1)}Br_{4.62(3)}I_{3.38(3)}$ (**III**), $Sn_{24}P_{19.1(1)}Br_{6.1(1)}I_{1.9(1)}$ (**IV**), and $Sn_{24}P_{19.6(1)}Br_8$ (**V**). The crystals of **II**, **III**, and **IV** were selected from the nonequilibrium reaction products of the first annealing at 825 K for 2 days of the nominal compositions $Sn_{24}P_{19.3}Br_4I_4$, $Sn_{24}P_{19.3}Br_5I_3$, and $Sn_{24}P_{19.3}Br_6I_2$, respectively. The crystals of **I** and **V** were prepared by chemical transport reactions method. Small amounts of the transport agent, tin(IV) iodide or mercury(II) bromide, were added to the preliminary synthesized samples with the compositions $Sn_{24}P_{19.3}Br_2I_6$ and $Sn_{24}P_{19.3}Br_8$, respectively. The mixtures were evacuated in silica ampules (150 mm, length; 7 mm, inner diameter) and sealed off. The ampules were placed in a horizontal furnace with a temperature gradient of 100 K (825/725 K). Single crystals of **I** and **V** suitable for structural investigation were found in the cold end of the ampules after about 5 days.

The compositions of the crystals **I**−**V** were calculated from the refined occupancies of atoms in the course of the crystal structure refinement. In the case of **II**, the iodine-to-bromine ratio was confirmed by the microprobe analysis, which showed the I/Br ratio, normalized to 8 halogen atoms in a formula unit, to be 2.3(1)/5.7-(1) which is in good agreement with X-ray crystal data, 2.35(3)/5.65(3). The same type of analysis confirmed the absence of mercury in **V**, which could have contaminated the crystal in the course of the chemical transport reaction (vide supra).

Single-Crystal X-ray Diffraction Experiments. Suitable single crystals of **I**−**IV** were mounted on a goniometer head of a CAD-4 (Nonius) diffractometer. The unit cell parameters were refined on the basis of 24 well-centered reflections in the angular range $11° < \theta < 14°$ and agreed well with those found from the powder data. The data were collected at room temperature and corrected for polarization and Lorenz effects. A semiempirical absorption correction was applied to the data on the basis of azimuthal scans of reflections having their χ angles close to 90°. The X-ray intensity data for crystal **V** were measured at 13 temperatures ranging from 90 to 293 K (Bruker KRYO-FLEX) on a Bruker SMART APEX CCD-based X-ray diffractometer system equipped with a Mo-target X-ray tube ($\lambda = 0.71073$ Å) operated at 1800 W power. A black block-shaped crystal of approximate dimensions 0.09 mm × 0.07 mm × 0.05 mm was mounted on a goniometer head with silicon grease (cyanoacrylate glue for the room temperature experiment). The detector was placed at a distance of 6.14 cm from the crystal. Before every data collection, the crystal was allowed to stand at the new temperature for at least 5 h. For each experiment, a total of 1850 frames were collected with a scan width of 0.3° in ω and an exposure time of 20 s/frame. The frames were integrated with the Bruker SAINT software package using a narrow-frame integration algorithm for a cubic unit cell to a maximum 2θ angle of 56.56° (0.75 Å resolution). The final cell constants are based upon the refinement of the XYZ-centroids of about 9000 reflections above $20\sigma(I)$. Analysis of the data showed negligible decay during data collection. Data were corrected for absorption effects using the empirical method (SADABS). The ratio of minimum to maximum apparent transmission was in the range 0.696−0.745 for different experiments. The data collection parameters are listed in Tables 1 and 2.

Crystal Structure Refinement. The crystal structures of **I**−**V** were solved in the space group $Pm\bar{3}n$ (No. 223) The atomic coordinates taken from tin phosphidiodide $Sn_{24}P_{19.3}I_8$ [12] were used as an initial model for crystal structure refinement with SHELXL-97 program package.[31]

The refinement of the crystal structure of **I** revealed the split in the Sn atomic position into two sites, Sn(1) and Sn(2), lying 0.58 Å apart, just as in the structure of $Sn_{24}P_{19.3}I_8$. The distance between the Sn(2) and P(2) atomic positions appeared to be very short (2.02 Å), while the P(2) atom had a large thermal displacement parameter. Two partially occupied tin atomic positions as well as the occupancy factor for the P(2) atom were then introduced into the anisotropic refinement, taking into account that there is no real Sn(2)−P(2) bonding of 2.02 Å, and these atoms alternate instead. Hence, the occupancy sum of Sn(2) and P(2) positions was fixed as unity, while the occupancy of Sn(1) was refined independently. It should be noted that after final refinement the occupancy sum of Sn(1) and Sn(2) positions appeared equal to unity within the accuracy of the refinement, and this sum was restrained in the final refinement. Refinement of the occupancy factors of the P(1) atomic position did not reveal any deviation from unity. Refinement of the occupancies of bromine and iodine atoms was performed independently for two halogen positions, 2a and 6d. In each position, the occupancy sum of bromine and iodine was fixed as unity.

The refinement procedure for the crystal structures of **II**−**IV** was essentially the same. In the case of **V**, the refinement of the occupancies of the halogen atomic position was apparently not performed, because of the absence of iodine. The crystal structure refinement parameters are given in Tables 1 and 2. It should be

(31) Sheldrik, G. M. *SHELXL-97, program for crystal structure refinement*; University of Göttingen: Göttingen, Germany, 1997.

Table 1. Crystallographic Data for **I**−**V**

	I	**II**	**III**	**IV**	**V**
chemical formula	$Sn_{24}P_{19.2(1)}Br_{2.35(3)}I_{5.65(3)}$	$Sn_{24}P_{19.1(1)}Br_{3.14(4)}I_{4.86(4)}$	$Sn_{24}P_{19.2(1)}Br_{4.62(3)}I_{3.38(3)}$	$Sn_{24}P_{19.1(1)}Br_{6.1(1)}I_{1.9(1)}$	$Sn_{24}P_{19.6(1)}Br_8$
fw	4347.96	4307.74	4241.29	4174.09	4094.85
space group	$Pm\bar{3}n$	$Pm\bar{3}n$	$Pm\bar{3}n$	$Pm\bar{3}n$	$Pm\bar{3}n$
a, Å	10.9200(10)	10.9140(10)	10.8860(10)	10.8440(10)	10.8142(7)
V, Å^3	1302.2(2)	1299.0(2)	1290.0(2)	1275.2(2)	1264.69(14)
Z	1	1	1	1	1
T, °C	20	20	20	20	20
λ, Å	0.71069	0.71069	0.71069	0.71069	0.71073
D_{calcd}, g cm^{-3}	5.545	5.507	5.459	5.436	5.377
μ, cm^{-1}	17.024	17.201	17.584	18.043	18.557
$R(F_o)^a$	0.0275	0.0211	0.0274	0.0386	0.0376
$R_w(F_o^2)^b$	0.0411	0.0372	0.0490	0.0629	0.0813

^{a} $R(F_o) = \sum||F_o| - |F_c||/\sum|F_o||$. ^{b} $R_w(F_o^2) = [\sum w(F_o^2 - F_c^2)^2/\sum w(F_o^2)^2]^{1/2}$, based on all data.

Table 2. Variable Temperature Crystallographic Data for **V**

T, °C	*a*, Å	*V*, Å^3	D_{calcd}, g cm^{-3}	*μ*, cm^{-1}	$R(F_o)^a$	$R_w(F_o^2)^b$
+20	10.8142(7)	1264.68(14)	5.377	18.557	0.0376	0.0813
−10	10.8123(5)	1264.02(9)	5.379	18.566	0.0368	0.0822
−20	10.8108(5)	1263.49(9)	5.382	18.574	0.0366	0.0821
−30	10.8098(4)	1263.14(8)	5.383	18.579	0.0374	0.0833
−45	10.8074(2)	1262.30(4)	5.387	18.591	0.0366	0.0839
−55	10.8067(2)	1262.06(4)	5.388	18.595	0.0372	0.0840
−60	10.8060(2)	1261.81(4)	5.389	18.598	0.0384	0.0863
−80	10.8027(2)	1260.66(4)	5.394	18.615	0.0369	0.0835
−100	10.8004(2)	1259.85(4)	5.397	18.627	0.0386	0.0865
−120	10.7987(2)	1259.26(4)	5.400	18.636	0.0374	0.0862
−140	10.7967(2)	1258.56(4)	5.403	18.646	0.0373	0.0862
−160	10.7945(2)	1257.79(4)	5.406	18.658	0.0372	0.0868
−183	10.7900(2)	1256.22(4)	5.413	18.681	0.0338	0.0788

^{a} $R(F_o) = \sum||F_o| - |F_c||/\sum|F_o||$. ^{b} $R_w(F_o^2) = [\sum w(F_o^2 - F_c^2)^2/\sum w(F_o^2)^2]^{1/2}$, based on all data.

noted that despite the fact that the amount of the phosphorus atoms in the obtained structures slightly differs, the general formula of all compounds obtained can be written as $Sn_{24}P_{19.3(2)}Br_xI_{8-x}$ taking into account the accuracy of occupancy determination for the P(2) position.

Results and Discussion

The analysis of the X-ray powder diffraction data shows that $Sn_{24}P_{19.3(2)}Br_xI_{8-x}$ ($x = 0-8$) is a solid solution within the whole composition range. It is isostructural to the previously reported tin phosphide iodide, $Sn_{24}P_{19.3}I_8$.[12] The powder X-ray patterns of the samples with different composition feature a systematic shift of peak positions. The dependence of the $Sn_{24}P_{19.3(2)}Br_xI_{8-x}$ solid solution cubic cell parameter upon the bromine content is given in Figure 2. The diagram has two principal features: (i) the dependence is nonlinear; (ii) the decrease in the value of the cubic cell parameter on going from $Sn_{24}P_{19.3}I_8$ to $Sn_{24}P_{19.3}Br_8$ is 0.14 Å (1.3%). The effect of nonlinearity in the clathrate unit cell parameter dependence was earlier observed by von Schnering and Menke[10] when they examined the cationic clathrates $Ge_{38}P_8Br_xI_{8-x}$ ($x = 2$, 4, and 6); however, no explanation was offered for the effect. The second feature points to an unusually high chemical compressibility of the cationic clathrate framework. For comparison, two pairs of the anionic type-I clathrates Cs_8Sn_{44} [32] versus K_8Sn_{44},[33] and $Sr_8Ga_{16}Ge_{30}$ [34] versus $Ba_8Ga_{16}Ge_{30}$,[23] might be considered. When substituting potassium with cesium (difference of two periods in periodic table), the cubic cell parameter changes by only 0.06 Å (0.6%), and when substituting barium with strontium (difference of one period, just as between bromine and iodine), the parameter difference is just 0.04 Å (0.4%). The example of the greater shrinkage is provided by the type-II clathrates. On going from $Cs_8Na_{16}Si_{136}$ to an almost guest-free Na_xSi_{136} clathrate, the unit cell parameter decreases by 0.13 Å (0.9%).[8] The comparison of these data with our results illustrates the striking difference in the clathrate framework compressibility. To explain the unusually high chemical compressibility of the cationic clathrate framework, as well as the nonlinear dependence of the unit cell parameter, we performed the X-ray single crystal experiments.

The crystal data reveal that the clathrate framework of $Sn_{24}P_{19.3(2)}Br_xI_{8-x}$ is built up of tin and phosphorus atoms. In the idealized structure, tin atoms occupying the 24*h* position of the space group $Pm\bar{3}n$ together with the P(1) atoms sitting in the 16*i* position build pentagonal dodecahedra, while the P(2) atoms residing in the 6*c* position link these polyhedra, thus completing tetrakaidecaedra. In such an arrangement (Figure 1), all atoms forming the polyhedral framework have tetrahedral coordination. In the actual structure, however, the occupancy of the P(2) atom position is about 55%, meaning that not all of the tetrakaidecahedra are complete. Besides, the position of tin atoms is split such that there are two alternative tin atoms, Sn(1) and Sn(2), partially occupying closely located 24*h* positions and, more importantly, having different environment. The Sn(1) is tetrahedrally coordinated by three phosphorus atoms and one tin atom, Sn(2). In turn, the Sn(2) exhibits the 3 + 3 environment of two phosphorus atoms and one tin atom, Sn(1), in the first coordination sphere plus three more distant tin atoms, Sn(2), in the second coordination sphere, with the Sn(2)−Sn(2) distance exceeding 3.15 Å. The analysis of the interatomic distances and valence angles in six crystals of $Sn_{24}P_{19.3(2)}Br_xI_{8-x}$ solid solution (crystals **I**−**V** and $Sn_{24}P_{19.3}I_8$ [12]) reveals that the Sn(1)−Sn(2), Sn(2)−Sn(2), and Sn(1)−P(1) distances decrease slightly on going from $x = 0$ to $x = 8$, while all other bonding distances and valence angles do not change within the accuracy of determination.

The halogen atoms are trapped in the cavities of the clathrate framework. There are two types of the cavities, the

(32) von Schnering, H. G.; Kröner, R.; Baitinger, M.; Peters, K.; Nesper, R.; Grin, Yu. *Z. Kristallogr.—New Cryst. Struct.* **2000**, *215*, 205.
(33) Zhao, J.-T.; Corbett, J. D. *Inorg. Chem.* **1994**, *33*, 5721−5726.
(34) Cohn, J. L.; Nolas, G. S.; Fessatidis, V.; Metcalf, T. H.; Slack, G. A. *Phys. Rev. Lett.* **1999**, *82*, 779−782.

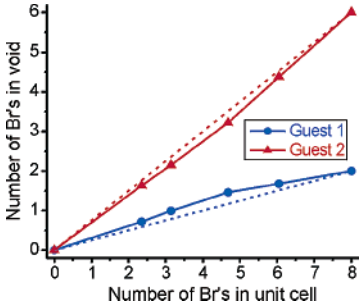

Figure 3. Distribution of the bromine atoms in the cages of $Sn_{24}P_{19.3(2)}Br_xI_{8-x}$ as a function of the bromine content. Dotted lines represent the ideal uniform distribution; solid lines are drawn to guide an eye. The esd's are smaller than the symbols used for the experimental data on this graph.

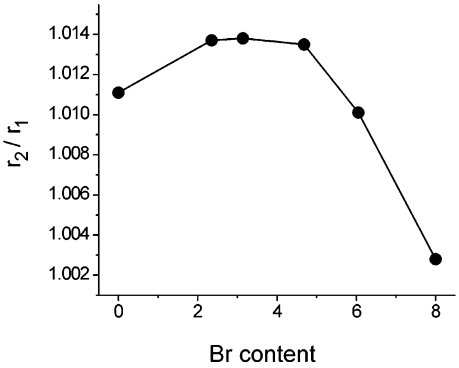

Figure 4. Dependence of the r_2/r_1 ratio of effective radii for the bigger and smaller cages on the bromine content in $Sn_{24}P_{19.3(2)}Br_xI_{8-x}$.

pentagonal dodecahedral and the tetrakaidecahedral, which occur in a 2:6 ratio in the unit cell and are centered by the 2*a* and 6*d* positions, respectively. Figure 3 shows that the guest bromine and iodine atoms mix in both cavities. The observed behavior is in sharp contrast with the earlier reported $Eu_2Ba_6M_8Si_{36}$ (M = Al, Ga).[19] In these compounds, having considerably more rigid clathrate framework than our solid solution, the europium and barium atoms exhibit complete ordering, occupying the smaller and bigger cages, respectively, of the clathrate-I framework. Figure 3 also shows that the actual distribution of the guest halogen atoms deviates slightly from the uniform distribution marked with dotted lines on the graph. It is clear, taking into account the accuracy of the determination of the occupancy factors of the guest atoms, that the bromine atoms have a slight preference for a smaller 20-vertex cage. This trend is most distinct near the medium bromine content ($x \approx 4$), suggesting that the features shown in Figures 2 and 3 may have the same origin. Despite such a preference, the complete filling of the smaller cages by bromine atoms only does not occur even in those cases where the number of bromine atoms in the structure considerably exceeds the number of these cages per unit cell.

The difference in the dimensions for the two types of the polyhedral cages, though it varies slightly with the bromine content, is noticeably small. The r_2/r_1 ratio, where r_2 and r_1 are the effective radii of the bigger and smaller cages, respectively, for the six structures (crystals **I**−**V** and $Sn_{24}P_{19.3}I_8$ [12]), is not far from unity, the highest ratio being 1.014 for **II** and the smallest, 1.003, for **V**. Such a small difference explains why the two guest atoms, Br^- and I^-, that possess different ionic radii, 1.96 and 2.20 Å,[35] respectively, occupy two types of cavities almost randomly. Figure 4 shows, however, that the r_2/r_1 dependence upon the bromine content has a "bell" shape. The small variation in the r_2/r_1 ratio seems to be responsible for the deviation from the uniform distribution of the bromine and iodine atoms among the cages of two different types, which is the most noticeable at the medium bromine content in agreement with the data shown in Figure 4.

It should be noted that the formalization of the title solid solution as $Sn_{24}P_{19.3(2)}Br_xI_{8-x}$ indicates that the phosphorus content may vary slightly. Indeed, the crystal data (Table 1) show that the refinement of the P(2) atom occupancy results in slightly different numbers. The question arises as to what extent such a difference could affect the unit cell parameters of the solid state solution? Our recent research[36] shows that the size of the cationic clathrates, in contrast to the anionic clathrates, is not sensitive to a small degree of the framework substitution and vacancy formation. For instance, the unit cell parameter decreases by only 0.01 Å on going from $Sn_{19.3}Cu_{4.7}As_{22}I_8$ to $Sn_{17.6}Cu_{6.4}As_{22}I_8$ and by 0.03 Å on going from $Sn_{20}Zn_4P_{20.8}I_8$ to $Sn_{17}Zn_7P_{22}I_8$ compared to the 0.13 Å increase on going from $Ba_8Ga_{16}Ge_{30}$ to $Ba_8Ga_{17.31}Ge_{25.90}Sb_{2.15}$,[37] where antimony atoms having greater radius intrude into the framework with concurrent formation of vacancies. In the title compounds, the possible deviation from stoichiometry is about 0.1 phosphorus atoms. This amount is below the accuracy of the microprobe analysis used in this work and is comparable with the accuracy of the phase analysis after the stoichiometric synthesis, as well as with the accuracy of the position occupancy refinement. Such a small, compared to the above-mentioned examples, deviation from the stoichiometry cannot affect substantially the unit cell parameter of the cationic clathrate. Therefore, we conclude that the type-I cationic clathrates differ strikingly from anionic clathrates in showing much greater compression in response to a chemical pressure imposed by the guest substitution and in being less sensitive to the framework substitutions.

We have demonstrated earlier[13] by the method of ab initio quantum-mechanical calculations that in the tin pnictideiodides the iodine atoms carry a high effective negative charge (up to −0.95 for the iodine atom inside the 24-vertex cage of $Sn_{24}P_{19.3}I_8$), so that the iodines can be considered as the I^- anions. Therefore, the electric conductivity in the cationic tin clathrates should occur through the framework, not involving the guest atoms, and it would seem reasonable that substitutions in the guest sublattice should not influence the conductivity properties. However, in the same work it was also shown that the states just below the Fermi level in $Sn_{24}P_{19.3}I_8$ are mainly composed of the 3+3-coordinated tin

(35) Shannon, R. D. *Acta Crystallogr.* **1976**, *A32*, 751−757.

(36) Shevelkov, A. V.; Zaikina, J. V.; Kovnir, K. A.; Reshetova, L. N. *Book of Abstracts*, 3rd National Conference on Crystal Chemistry, Chernogolovka, Moscow Region, May 2003; pp 151−152.

(37) Latturner, S. E.; Bryan, J. D.; Blake, N.; Metiu, H.; Stucky, G. D. *Inorg. Chem.* **2002**, *41*, 3956−3961.

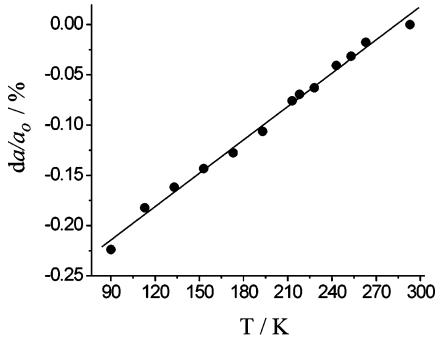

Figure 5. Linear contraction of **V**. Filled circles (●), experimental data; line (—), linear fit.

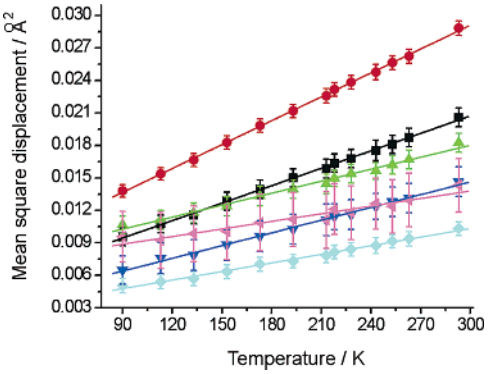

Figure 6. Temperature dependence of the atomic displacement parameters (ADPs) for crystallographically independent atoms in the structure of **V**. Br(1), black; Br(2), red; Sn(1), green; Sn(2), blue; P(1), cyan; P(2), magenta. Corresponding linear fits are shown with the same color.

atoms and that namely these atoms are responsible for the conductivity properties. We show in this work that the substitution of bromine for iodine in the $Sn_{24}P_{19.3}I_8$ results in shortening of the tin−tin distances in the clathrate framework and, consequently, in changes in the local environment of the 3+3-coordinated tin atom, Sn(2). The Sn(2)−Sn(1) and Sn(2)−Sn(2) bond distances become shorter by 0.05 and 0.08 Å, respectively. It is not clear if such shortening can affect the transport properties of the tin-based cationic clathrates. However, we demonstrated earlier[12] that $Sn_{24}P_{19.3}I_8$ is already a narrow gap semiconductor, $E_g \approx 0.04$ eV, and in this work we confirm that substitution of iodine by bromine does not induce the insulator-to-metal transition. In addition, it should be taken into account that the phosphorus content differs within the experimental error from one sample of the title solid solution to another. This seems to be a very important feature since the concentration of vacancies strictly corresponds to the number of the 3+3-coordinated tin atoms in the clathrate framework. As it was found earlier for some anionic clathrates,[18] the slight variation in composition of the clathrate framework may lead to the changes in their transport properties. It might as well affect the magnetic properties, though our preliminary measurements performed on the samples with $x = 2$, 3, and 6 indicate that the phases are diamagnetic. These observations require further investigation.

The subject under discussion in the literature is what causes the glasslike thermal conductivity of the clathrates? It is generally believed[17] that the "rattling" of the guest atoms in the oversized cages scatter resonantly the heat-carrying acoustic phonons thus leading to glasslike heat conduction. However, recent reports[18,23] suggest that the role of the "rattling" is overestimated. Alternatively, the guest 6*d* position split into a set of nearby positions is proposed[22,25−27] to reduce thermal conductivity due to the scattering from the guest atom tunneling between the split states.[18] In this work, we address two questions: (i) Is the *6d* position split in cationic clathrates, and (ii) are these clathrates prospective thermoelectric materials due to a low thermal conductivity? To answer this, we performed the temperature-dependent investigation for the structure of **V**. No phase transition was detected in the temperature range 90−293 K, and the linear contraction (Figure 5) is comparable with those observed for anionic clathrates.[27] It is also found that at either temperature the structure of **V** is best solved with the single 6*d* Br(2) site. All attempts to solve the structure with the split-site model and the partially occupied 24*j*, 24*k*, or 12*h* positions led to the significant increase in *R*-values as well as to the substantial remaining electron density exactly at the 6*d* site.

The temperature dependence of the atomic displacement parameters (ADP) for all atoms in structure **V** is shown in Figure 6. It is clear from drawings that all dependencies are linear and the ADP of the Br(2) is larger than those for the other atoms. It is known from literature[38] that the linear dependencies of ADPs can be used for estimation of the Debye temperature, θ_D, since the slope of the $\langle u^2 \rangle = f(T)$ function is expressed as $3h^2/(4\pi^2 M \theta_D^2 k_B)$, where M is the average atomic mass and $\langle u^2 \rangle$ is the mean square atomic displacement. Using this expression and the results of the linear fits (Figure 6), we can estimate θ_D as 220 K.

The lattice contribution to the thermal conductivity is expressed as

$$\kappa_l = C_v v_s \lambda \qquad (1)$$

where C_v is the heat capacity per unit volume, v_s is the mean phonon velocity, and λ is the mean free path of the phonons.[39] The Debye model relates the mean phonon velocity and the Debye temperature as $v_s = [(\theta_D k_B 2\pi)/h]/[6\pi^2(N/V)]^{1/3}$, where N/V is the number of atoms per unit volume.[40] Given the Debye temperature, we calculated $v_s = 2170$ m/s. Since the Debye temperature is approximately 220 K, the heat capacity can be estimated by the Dulong−Petit law,[39] according to which $C_v = 24.93n$ J/(mol K), well above the Debye temperature, where n is the number of atoms per formula. For the $Sn_{24}P_{19.6}Br_8$ this gives $C_v = 0.17 \times 10^7$ J/(m^3 K). The estimation of the mean free path of the phonons is the most difficult. As there is no sign of the 6*d* site split, we assume that λ is the distance between the "rattlers"[38] (the Br(2) atoms occupying the 6*d* position) that is equal to 5.4×10^{-10} m. Using eq 1 we can now estimate the lattice part of the thermal conductivity as $\kappa_l = 0.7$ W/(m K).

(38) Sales, B. C.; Chakoumakos, B. C.; Mandrus, D.; Sharp, J. W. *J. Solid State Chem.* **1999**, *146*, 528−532.
(39) White, M. A. *Properties of Materials*; Oxford University Press: Oxford, 1999.
(40) Fistul, V. I. *Physics and Chemistry of Solids*; Metallurgia Press: Moscow, 1995.

Here we performed a rough estimation of the lattice part of the thermal conductivity; however, the similar procedure was proved[27,38] to give a good agreement between the estimated and measured values for different compounds described as having "rattling" atoms. Also, it was previously shown[18,34,41] that the lattice part constitutes 95−98% of the total thermal conductivity; hence, the value of κ_l gives rather good estimation of this property. The remaining 2−5% is the electronic part of thermal conductivity, which depends on the properties of the clathrate framework, such as vacancy concentration and/or nature of a substituting element, but never plays a dominating role unless the compound exhibits metallic conductivity.[39] Though the origin of low, glasslike thermal conductivity in clathrates is still a matter of discussion,[42] the overall result of this work shows that the value of κ_l for the title phase is comparable with the values experimentally obtained for various anionic clathrates.[22,24,29,43] Thus, it can be proposed that the cationic tin clathrates are good candidates for developing novel thermoelectric materials based on the "phonon glass, electron crystal" concept.

Acknowledgment. Authors wish to thank Dr. P. E. Kazin for the magnetization measurements and Dr. M. G. Novozhilov for the microprobe analyses. This research is supported by Russian Foundation for Basic Research, Grant 03-03-32514a, U.S. Civilian Research & Development Foundation for the Independent States of the Former Soviet Union, Award 12735, and European Commission 5th Framework Program, Contract HPRN-CT-2002-00193. E.V.D. is grateful to the Faculty Research Award Program and to the National Science Foundation for funding CCD diffractometer (CHE-0130985) at University at Albany. A.V.S. thanks Russian Science Support Foundation for the research award.

Supporting Information Available: CIF file containing information on the 16 structural experiments. This material is available free of charge via the Internet at http://pubs.acs.org.

IC035097F

(41) Keppens, V.; Mandrus, D.; Sales, B. C.; Chakoumakos, B. C.; Dai, P.; Coldea, R.; Maples, M. B.; Gajewski, D. A.; Freeman, E. J.; Bennington, S. *Nature* **1998**, *395*, 876−878.

(42) Bentien, A.; Christensen, M.; Bryan, J. D.; Sanchez, A.; Paschen, S.; Steglich, F.; Stucky, G. D.; Iversen, B. B. *Phys. Rev.* **2004**, *69*, 045107/1−045107/5.

(43) Nolas, G. S.; Weakley, T. J. R.; Cohn, J. L. *Chem. Mater*. **1999**, *11*, 2470−2473.